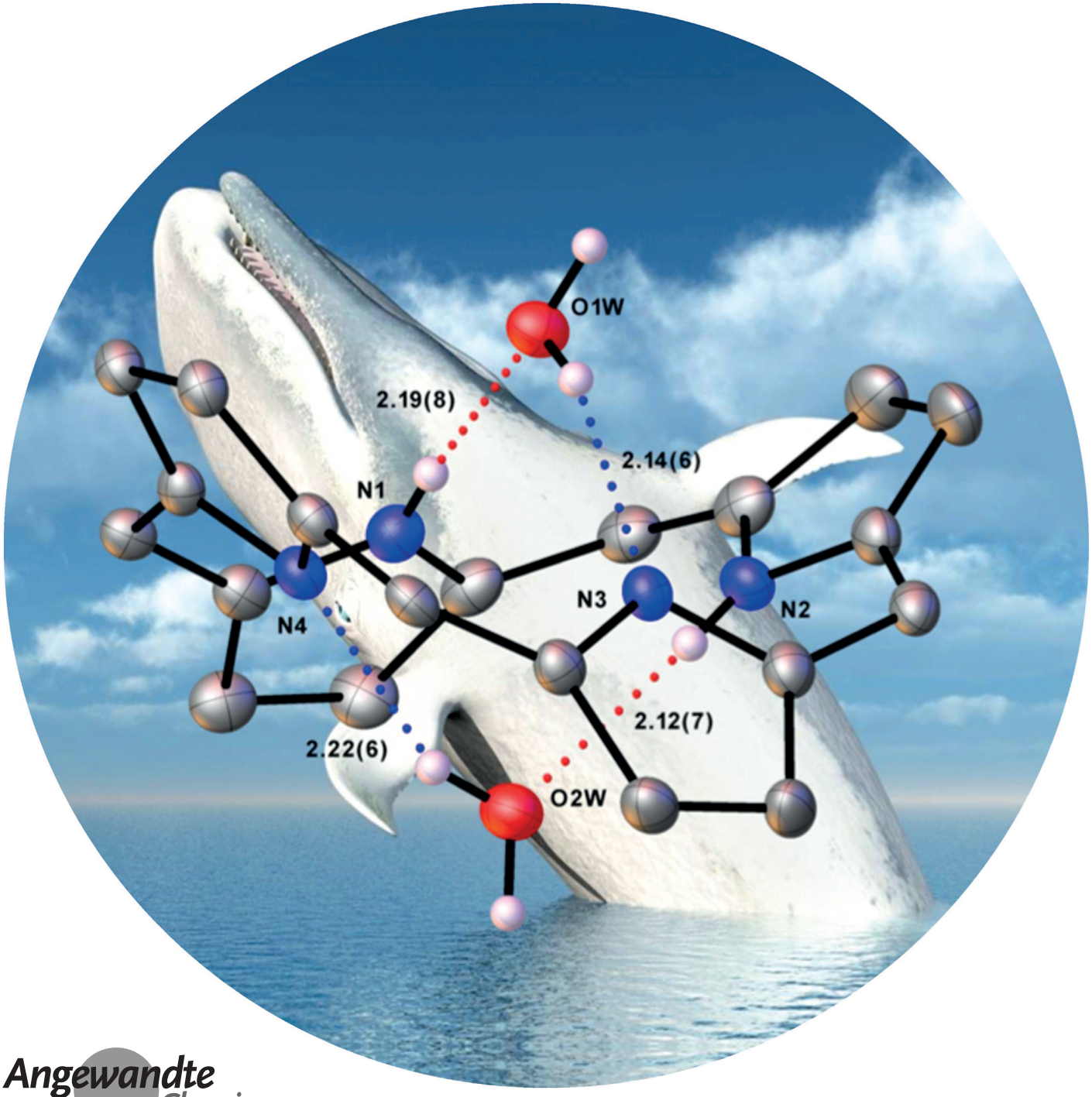
Porphyrin Tautomerism

International Edition: DOI: 10.1002/anie.201701965
German Edition: DOI: 10.1002/ange.201701965

Stabilization and Structure of the *cis* Tautomer of a Free-Base Porphyrin

*Kolle E. Thomas, Laura J. McCormick, Hugo Vazquez-Lima, and Abhik Ghosh**

Dedicated to Professor Roald Hoffmann on the occasion of his 80th birthday



© 2017 Wiley-VCH Verlag GmbH & Co. KGaA, Weinheim

Abstract: *Single-crystal X-ray analysis of the β-heptakis(trifluoromethyl)-meso-tetrakis(p-fluorophenyl)porphyrin, H_2-[$(CF_3)_7$TpFPP], has revealed the first example of a stable cis tautomer of a free-base porphyrin, the long-postulated intermediate of porphyrin tautomerism. The stability of the unique molecule appears to reflect a dual origin: a strongly saddled porphyrin skeleton, which alleviates electrostatic repulsion between the two NH protons, and two polarization-enhanced, transannular N–H···O–H···N hydrogen bond chains, each involving a molecule of water. DFT calculations suggest that the observed tautomer has a lower energy than the alternative, doubly hydrated trans tautomer by some 8.3 kcal mol^{-1}. A fascinating prospect thus exists that H_2[$(CF_3)_7$TpFPP]·2 H_2O and cognate structures may act as supramolecular synthons, which, given their chirality, may even be amenable to resolution into optically pure enantiomers.*

The fundamental geometrical disposition and dynamics of the central NH protons of free-base porphyrins were elucidated in a series of seminal studies during the latter part of the last century.[1] Early X-ray[2–5] crystal structures and ab initio calculations[6–8] confirmed a linear N–H···H–N arrangement with each NH proton engaged in symmetric, bifurcated hydrogen bonding with two neighboring nitrogen atoms. Detailed kinetic studies further established that the degenerate tautomerism of free-base porphyrins occurs asynchronously, most likely via the *cis* free-base tautomer.[9–12] Ab initio and density functional theory (DFT) calculations established the *cis* tautomer as a true minimum, with exact C_{2v} symmetry for unsubstituted porphyrin.[13,14] No direct, experimental characterization of the *cis* tautomer, however, has been reported until now. Here we describe the serendipitous isolation and single-crystal X-ray structure determination of the *cis* tautomer of a free-base porphyrin. The structure reveals an unusual combination of factors that result in the existence of the *cis* tautomer as the energetically preferred form for the free-base porphyrin in question.

In the course of our continuing studies of electron-deficient, highly perfluoroalkylated porphyrinoid systems,[15–17] acid-induced demetalation of an inseparable mixture of Cu[$(CF_3)_7$TpFPP] and Cu[$(CF_3)_8$TpFPP] led to the corresponding free-base porphyrins H_2[$(CF_3)_7$TpFPP] and H_2[$(CF_3)_8$TpFPP], which could be readily separated by means of column chromatography.[18] Of the two products, H_2-[$(CF_3)_7$TpFPP] proved amenable to single-crystal X-ray structure analysis, revealing the first example of a stable, *cis* tautomer of a free-base porphyrin (Figure 1 and Table 1 and Table 2). As expected on the basis of its sterically hindered character,[19–21] the porphyrin core is strongly saddled, with the two central NH groups pointing above and below the mean N_4 plane. Each NH group acts as a hydrogen bond donor to a water molecule, which in turn acts as a hydrogen bond donor

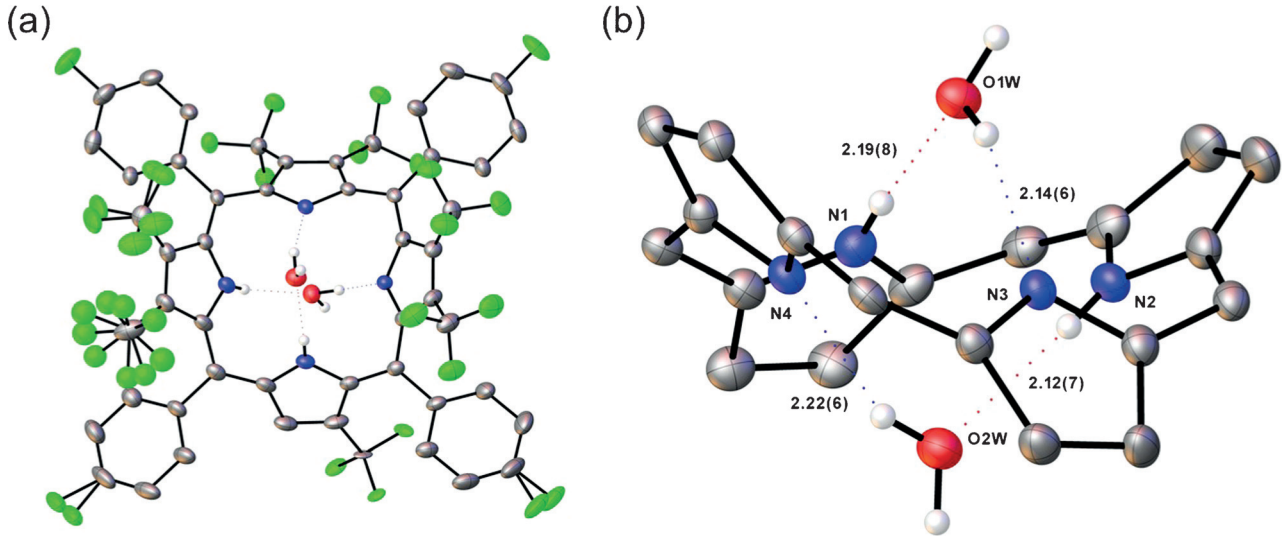


Figure 1. Thermal ellipsoid plots (33 %) of H_2[$(CF_3)_7$TpFPP]·2 H_2O: a) top view and b) close-up of the porphyrin core with hydrogen bond distances [Å].

[*] Dr. K. E. Thomas, Dr. H. Vazquez-Lima, Prof. Dr. A. Ghosh
Department of Chemistry
UiT—The Arctic University of Norway, 9037 Tromsø (Norway)
E-mail: abhik.ghosh@uit.no
Dr. L. J. McCormick
Advanced Light Source, Lawrence Berkeley National Laboratory
Berkeley, CA 94720-8229 (USA)

Supporting information, including details of spectroscopic and crystallographic data, and the ORCID identification number(s) for the author(s) of this article can be found under: http://dx.doi.org/10.1002/anie.201701965.

to an unprotonated nitrogen across the porphyrin. Both the N–H···O and O–H···N hydrogen bonds are approximately linear and 2.1–2.2 Å in length.[22–27] Figure 2 shows the location of the peaks of electron density corresponding to the N- and O-bound hydrogen atoms. The assignment and modeling of hydrogen atom positions is described in detail in the Supporting Information.

The unique stability of the *cis* tautomer appears to result from a dual origin, comprising both strong saddling and the hydrogen bond network. By increasing their spatial separa-

 © 2017 Wiley-VCH Verlag GmbH & Co. KGaA, Weinheim

Table 1: Crystal and structure refinement data for H_2-[$(CF_3)_7$TpFPP]·2 H_2O.

Chemical Formula	$C_{51}H_{23}F_{25}N_4O_2$
Formula mass	1198.73
Crystal system	monoclinic
Space group	$P2_1/c$
λ [Å]	0.7749
a [Å]	14.3852(11)
b [Å]	27.9206(18)
c [Å]	11.9969(11)
α [°]	90
β [°]	104.213(6)
γ [°]	90
Z	4
V [Å^3]	4671.0(6)
T [K]	100(2)
ρ [g cm^{-3}]	1.705
Measured reflections	36249
Unique reflections	7439
Parameters	840
Restraints	56
R_{int}	0.0398
θ range [°]	2.068–26.566
$R1$, $wR2$ all data	0.1103, 0.2762
S (GooF) all data	1.042
Max/min res. Dens. [e Å^{-3}]	1.452/−1.123

Table 2: Hydrogen bond metrical parameters [Å,°] for $H_2[(CF_3)_7TpFPP]$.

D−H···A	d(D−H)	d(H···A)	d(D···A)	∠DHA
N(2)-H(2)···O(2W)	0.73(6)	2.12(7)	2.847(6)	177(7)
O(2W)-H(3W)···N(4)	0.82(5)	2.22(6)	2.983(6)	156(8)
N(1)-H(1)···O(1W)	0.70(7)	2.19(8)	2.873(7)	166(8)
O(1W)-H(2W)···N(3)	0.84(5)	2.14(6)	2.909(6)	153(9)

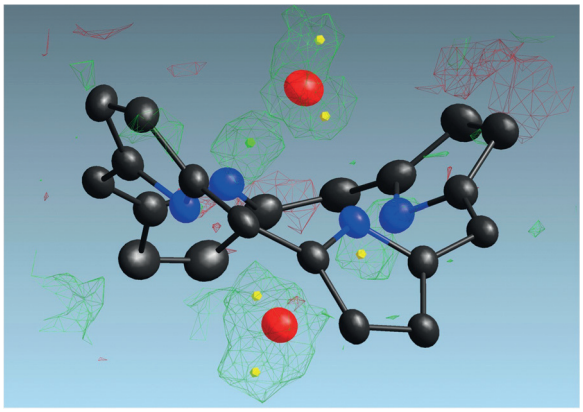


Figure 2. Electron density map surrounding the central porphyrin unit of $H_2[(CF_3)_7TpFPP]·2H_2O$. Peripheral CF_3 and C_6H_4F groups have been omitted for clarity. The threshold for the electron density map has been set at 0.2 e Å^{-3}. The yellow and green solid polyhedral represent peaks of electron density. The $F_{observed}-F_{calculated}$ electron density map is shown as either green or red polyhedral surfaces for positive and negative $F_{obs}-F_{calc}$ values, respectively.

tion, strong saddling alleviates the electrostatic repulsion between the central NH protons of the *cis* tautomer. Additional stability accrues from two so-called homodromic,[24,25,28,29] polarization-enhanced N−H···O−H···N hydrogen bond chains. DFT calculations (PBE0[30,31]-D3/STO-TZ2P; ADF[32] 2016) calculations on the *cis* and *trans* tautomers of a series of free-base porphyrins[33] are consistent with the dual stabilization of the *cis* tautomer (Table 3). (The term homodromic refers to a hydrogen-bonded chain or ring where the constituent D−H···A units all have the same directionality.) Thus, the energy of the *cis* tautomer relative to the *trans* tautomer (in kcal mol^{-1}) decreases along the series H_2[TPP] (8.2), $H_2[Br_8TPP]$ (5.1), $H_2[I_8TPP]$ (4.9),[34] and $H_2[(CF_3)_8TPP]$ (1.1), paralleling the steep increase in saddling of the optimized structures. Hydrogen bonding with two water molecules then tips the energy balance, favoring the *cis* tautomer for $H_2[(CF_3)_8TPP]·2H_2O$ by 8.3 kcal mol^{-1} relative to the *trans* tautomer. As elsewhere,[24,25] the homodromic hydrogen bond network found in the *cis* tautomer appears to confer much greater stability than the antidromic network assumed for the *trans* tautomer.

The calculated stability of the *cis* tautomer of H_2-[$(CF_3)_8$TPP]·2 H_2O by a clear margin of energy potentially presages the emergence of *cis* porphyrin dihydrates as a new supramolecular synthon.[35,36] Furthermore, the chiral, approximately C_2-symmetric nature of the compounds may allow successful resolution of the enantiomers, ushering in a new, inherently chiral chromophore.[37,38] Another interesting aspect of $H_2[(CF_3)_7TpFPP]$ and $H_2[(CF_3)_8TpFPP]$ is that both molecules exhibit strong Q bands extending well into the NIR region (see Figure S3 in the Supporting Information), potentially suggesting applications in photodynamic therapy and as NIR dyes.[39]

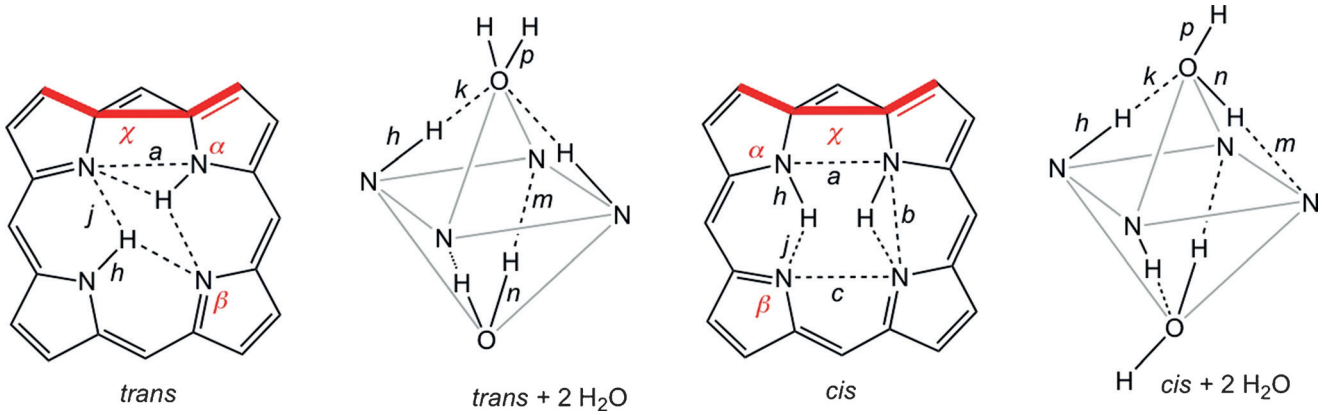
In conclusion, a detailed X-ray analysis of β-heptakis(trifluoromethyl)-*meso*-tetrakis(*p*-fluorophenyl)porphyrin, H_2-[$(CF_3)_7$TpFPP], has yielded unambiguous proof of the existence of a long-postulated reactive intermediate—the *cis* tautomer of a free-base porphyrin. The stability of the unique molecule has a dual origin, namely, a strongly saddled geometry and a hydrogen bond network involving two water molecules of crystallization per porphyrin unit.

Experimental Section

Synthetic protocols and spectroscopic data (remove reference) have been presented in the Supporting Information, with the present section focusing on the X-ray structure analysis.[44] X-ray data for $H_2[(CF_3)_7TpFPP]·2H_2O$ were collected on beamline 11.3.1 at the Advanced Light Source, using a Bruker D8 diffractometer equipped with a PHOTON100 CMOS detector operating in shutterless mode. The crystal was coated in protective oil prior to being mounted on a MiTeGen® kapton micromount and placed under a nitrogen stream at 100(2) K provided by an Oxford Cryostream 800 Plus low-temperature apparatus. Diffraction data were collected with synchrotron radiation monochromated using silicon(111) to a wavelength of 0.7749(1) Å. An approximate full-sphere of data was collected using a combination of ϕ and ω scans with scan speeds of 1 second for 4 degrees for the ϕ scans, and 1 second per degree for the ω scans at $2\theta = 0$ and −45, respectively. The structures were solved by intrinsic phasing (SHELXT)[40] and refined by full-matrix least squares on F^2 (SHELXL-2014).[41] Absorption corrections were applied using SADABS.[42] Additional crystallographic information has been summarized in Table 1 and Table 2, and full details can be found in the

 © 2017 Wiley-VCH Verlag GmbH & Co. KGaA, Weinheim

Table 3: Selected PBE0 and experimental geometry parameters [Å,deg]; relative energies [kcal mol^{-1}] of the *cis* tautomers.[a]



Molecule	trans χ	α	β	a	j	cis χ	α	β	a	b	c	j	E_{cis}
H_2[TPP]	13.9	110.7	105.6	2.915	2.303	3.3	110.3	105.9	3.170	2.697	3.083	1.914	8.2
H_2[Br_8TPP]	63.6	112.8	107.6	2.913	2.351	74.8	112.5	107.7	3.042	2.864	3.009	2.378	5.1
H_2[I_8TPP]	71.9	112.7	107.5	2.906	2.377	84.8	112.3	107.5	3.027	2.876	2.994	2.431	4.9
H_2[$(CF_3)_8$TPP]	129.6	113.2	107.6	2.979	2.735	134.1	112.9	107.3	3.049	2.956	2.981	2.726	1.1
H_2[$(CF_3)_8$TPP]·2 H_2O	133.8	112.4	107.6	2.988	2.786	132.6	111.9	107.3	3.070	3.033	3.010	2.778	−8.3
H_2[$(CF_3)_7$TPP]·2 H_2O (expt)						117.6(11)	110.7(5), 111.3(5)	108.7(4), 107.8(4)	3.047(7)	3.011(6), 3.053(6)	2.992(5)		

[a] Additional PBE0 hydrogen bond metrical parameters [Å] for the two tautomers of H_2[$(CF_3)_8$TPP]·2 H_2O.

trans h	k	m	n	p	cis h	k	m	n	p
1.017	2.072	2.114	0.967	0.964	1.031	1.831	1.971	0.981	0.959

crystallographic information files provided in the Supporting Information.

All full-occupancy non-hydrogen atoms were refined anisotropically. A detailed discussion of the disorder of the CF_3 groups and the modeling of the N- and O-bound hydrogen atoms is included in the Supporting Information. Hydrogen atoms attached to the carbon atoms belonging to the porphyrin unit were included at their geometrically estimated positions and refined as riding atoms. Once the final model of the porphyrin unit was obtained, peaks of electron density corresponding to the location of the hydrogen atoms belonging to the porphyrin pyrrole groups and water molecules of crystallization were observed. Electron density maps generated using shelXle[43] (Figure 2) show that electron density is localized around two *cis* porphyrin nitrogen atoms (namely N1 and N2). Finally, note that each H_2[$(CF_3)_7$TpFPP]·2 H_2O unit is chiral and that there are four such, symmetry-related units, two of each handedness, within each unit cell (Figure 3). The porphyrin units are organized into layers such that all the units within a given layer have the same handedness.

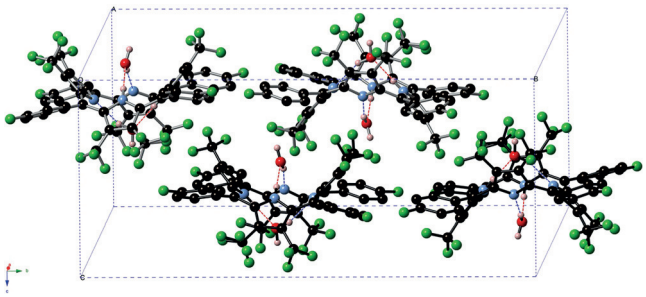


Figure 3. Unit cell of H_2[$(CF_3)_7$TpFPP]·2 H_2O.

Acknowledgements

This work was supported by grants 231086 and 262229 of the Research Council of Norway (AG). This research also used resources of the Advanced Light Source, which is a DOE Office of Science User Facility under contract number DE-AC02-05CH11231.

Conflict of interest

The authors declare no conflict of interest.

Keywords: hydrogen bonding · porphyrins · supramolecular chemistry · tautomers · X-ray diffraction

How to cite: *Angew. Chem. Int. Ed.* **2017**, *56*, 10088–10092
Angew. Chem. **2017**, *129*, 10222–10226

[1] H. H. Limbach, J. M. Lopez, M. Kohen, *Philos. Trans. R. Soc. London Ser. B* **2006**, *361*, 1399–1415.
[2] S. J. Silvers, A. Tulinsky, *J. Am. Chem. Soc.* **1967**, *89*, 3331–3337.
[3] P. W. Codding, A. Tulinsky, *J. Am. Chem. Soc.* **1972**, *94*, 4151–4157.
[4] B. M. L. Chen, A. Tulinsky, *J. Am. Chem. Soc.* **1972**, *94*, 4144–4151.
[5] A. Tulinsky, *Ann. N. Y. Acad. Sci.* **1973**, *206*, 47–69.
[6] J. Almlöf, *Int. J. Quantum Chem.* **1974**, *8*, 915–924.
[7] A. Ghosh, J. Almlöf, P. G. Gassman, *Chem. Phys. Lett.* **1991**, *186*, 113–118.

 © 2017 Wiley-VCH Verlag GmbH & Co. KGaA, Weinheim

[8] J. Almlöf, T. H. Fischer, P. G. Gassman, A. Ghosh, M. Häser, *J. Phys. Chem.* **1993**, *97*, 10964 – 10970.
[9] T. J. Butenhoff, C. B. Moore, *J. Am. Chem. Soc.* **1988**, *110*, 8336 – 8341.
[10] T. Butenhoff, R. Chuck, H.-H. Limbach, C. B. Moore, *J. Phys. Chem.* **1990**, *94*, 7847 – 7851.
[11] H.-H. Limbach, J. Hennig, D. Gerritzen, H. Rumpel, *Faraday Discuss. Chem. Soc.* **1982**, *74*, 229 – 243.
[12] J. Braun, M. Schlabach, B. Wehrle, M. Köcher, E. Vogel, H.-H. Limbach, *J. Am. Chem. Soc.* **1994**, *116*, 6593 – 6604.
[13] A. Ghosh, J. Almlöf, *J. Phys. Chem.* **1995**, *99*, 1073 – 1075.
[14] D. K. Maity, R. L. Bell, T. N. Truong, *J. Am. Chem. Soc.* **2000**, *122*, 897 – 906.
[15] K. E. Thomas, I. H. Wasbotten, A. Ghosh, *Inorg. Chem.* **2008**, *47*, 10469 – 10478.
[16] K. E. Thomas, J. Conradie, L. K. Hansen, A. Ghosh, *Eur. J. Inorg. Chem.* **2011**, 1865 – 1870.
[17] K. E. Thomas, C. M. Beavers, A. Ghosh, *Mol. Phys.* **2012**, *110*, 2439 – 2444.
[18] Abbreviations: TpFPP = *meso*-tetrakis(*p*-fluorophenyl)porphyrin; $(CF_3)_{7/8}$ denotes β-heptakis/octakis(trifluoromethyl) substitution.
[19] J. A. Shelnutt, X.-Z. Song, J.-G. Ma, S.-L. Jia, W. Jentzen, C. J. Medforth, *Chem. Soc. Rev.* **1998**, *27*, 31 – 42.
[20] C. J. Medforth, M. O. Senge, K. M. Smith, L. D. Sparks, J. A. Shelnutt, *J. Am. Chem. Soc.* **1992**, *114*, 9859 – 9869.
[21] I. V. Sazanovich, V. A. Galievsky, A. van Hoek, T. J. Schaafsma, V. L. Malinovskii, D. Holten, V. S. Chirvony, *J. Phys. Chem. B* **2001**, *105*, 7818 – 7829.
[22] C. L. Perrin, J. B. Nielson, *Annu. Rev. Phys. Chem.* **1997**, *48*, 511 – 544.
[23] G. A. Jeffrey, *An Introduction to Hydrogen Bonding*, Oxford University Press, Oxford, **1997**.
[24] S. Scheiner, *Hydrogen Bonding: A Theoretical Perspective*, Oxford University Press, Oxford, **1997**.
[25] T. Steiner, *Angew. Chem. Int. Ed.* **2002**, *41*, 48 – 76; *Angew. Chem.* **2002**, *114*, 50 – 80.
[26] Y. Marechal, *The Hydrogen Bond and the Water Molecule*, Elsevier, Amsterdam, **2006**.
[27] An explanatory note may be in order on the short N-H distances, 0.73(6) and 0.70(7) Å, observed here. Although it is customary to restrain N–H bond distances to 0.88 Å or 0.91 Å at 100 K, we have not done so here, in order to underscore that the NH hydrogens were assigned and refined in their current positions and that no attempts have been made to influence their relative positions.
[28] W. Saenger, *Nature* **1979**, *279*, 343 – 344.
[29] W. Saenger, K. Lindner, *Angew. Chem. Int. Ed. Engl.* **1980**, *19*, 398 – 399; *Angew. Chem.* **1980**, *92*, 404 – 405.
[30] a) J. P. Perdew, K. Burke, M. Ernzerhof, *Phys. Rev. Lett.* **1996**, *77*, 3865 – 3868; b) J. P. Perdew, K. Burke, M. Ernzerhof, *Phys. Rev. Lett.* **1997**, *78*, 1396 – 1396; c) J. P. Perdew, M. Ernzerhof, K. Burke, *J. Chem. Phys.* **1996**, *105*, 9982 – 9985.
[31] F. Weigenda, R. Ahlrichs, *Phys. Chem. Chem. Phys.* **2005**, *7*, 3297 – 3305.
[32] a) G. te Velde, F. M. Bickelhaupt, S. J. A. van Gisbergen, C. Fonseca Guerra, E. J. Baerends, J. G. Snijders, T. Ziegler, *J. Comput. Chem.* **2001**, *22*, 931 – 967; b) C. Fonseca Guerra, J. G. Snijders, G. te Velde, E. J. Baerends, *Theor. Chem. Acc.* **1998**, *99*, 391 – 403.
[33] The PBE0 hybrid functional has often been used to study hydrogen-bonded systems. The results obtained, particularly the energetics and key geometry parameters, here were also checked against those obtained with other functionals such as OLYP and B3LYP; no significant differences between the different functionals could be discerned.
[34] I. K. Thomassen, H. Vazquez-Lima, K. J. Gagnon, A. Ghosh, *Inorg. Chem.* **2015**, *54*, 11493 – 11497.
[35] G. R. Desiraju, *Angew. Chem. Int. Ed. Engl.* **1995**, *34*, 2311 – 2327; *Angew. Chem.* **1995**, *107*, 2541 – 2558.
[36] G. R. Desiraju, J. J. Vittal, A. Ramanan, *Crystal Engineering: A Textbook*, World Scientific, Singapore, **2011**.
[37] A. Moscowitz, *Adv. Chem. Phys.* **1962**, *4*, 67 – 112.
[38] For a recent review of inherently chiral chromophores, see: M. Kwit, P. Skowronek, J. Gawronski, J. Frelek, M. Woznica, A. Butkiewicz in *Comprehensive Chiroptical Spectroscopy*, *Vol. 2* (Eds.: N. Berova, P. L. Polavarapu, K. Nakanishi, R. W. Woody), Wiley, Hoboken, **2012**, chap. 2, pp. 39 – 72.
[39] M. Ethirajan, Y. Chen, P. Joshi, R. K. Pandey, *Chem. Soc. Rev.* **2011**, *40*, 340 – 362.
[40] G. M. Sheldrick, *Acta Crystallogr. Sect. A* **2015**, *71*, 3 – 8.
[41] G. M. Sheldrick, *Acta Crystallogr. Sect. C* **2015**, *71*, 3 – 8.
[42] SADABS: Area-Detector Absorption Correction; Siemens Industrial Automation, Inc.: Madison, WI, **1996**.
[43] C. B. Hübschle, G. M. Sheldrick, B. Dittrich, *J. Appl. Crystallogr.* **2011**, *44*, 1281 – 1284.
[44] Supplementary crystallographic data for this paper are given in CCDC 1501215. These data can be obtained free of charge from The Cambridge Crystallographic Data Centre.

Manuscript received: February 22, 2017
Version of record online: March 29, 2017

 © 2017 Wiley-VCH Verlag GmbH & Co. KGaA, Weinheim